

Foundations of Quantum Physics

April 26, 2024

A Realizable, Non-Null Schrödinger's Cat Experiment

Martin S. Altschul*

*Northwest Permanente
Salem, Oregon 97306*

Brett D. Altschul†

*Department of Physics
Massachusetts Institute of Technology
Cambridge, Massachusetts 02139*

Abstract

Working from the Schrödinger's Cat paradigm, a series of experiments are constructed. The Bedford-Wang experiment is examined, and the ambiguity in its meaning is addressed. We eliminate this ambiguity by abandoning the idea of the triggering event, replacing the two-state system with a mirror that undergoes wave packet spreading. This creates an experimentally testable version of a modified Schrödinger's Cat experiment for which a null result is not the obvious outcome.

*altschulma@kpnwoa.mts.kpnw.org

†baltschu@mit.edu

I. INTRODUCTION

Twenty years ago Bedford and Wang (BW) [1,2] devised an experimentally realizable version of the Schrödinger’s Cat (SC) experiment. They started with an ordinary double slit experiment using photons of wavelength λ_1 ; they then added a refinement. The slits have movable slit covers that allow two possible configurations:

1. Configuration Ab has slit A open and slit B closed.
2. Configuration aB has slit A closed and slit B open.

The slit control system is triggered by photocells registering the output of a beam splitter. In this way, the slit system (SS) can be set up so that its state vector is entirely determined by a single photon processed by the beam splitter/photocell system. BW claim that if the beam splitter outputs a photon in a 50/50 superposition state, then further application of the superposition principle (SP) according to the standard interpretation of quantum mechanics (SIQM) forces us to conclude that the slit system is in the state

$$|\psi\rangle = \frac{1}{\sqrt{2}}(|Ab\rangle + |aB\rangle), \quad (1)$$

and consequently, a double slit interference pattern is to be expected (Figure 1).

BW then add that “although the result seemed a foregone conclusion” the experiment was performed and yielded a null result—no double slit interference. But is this result interesting or informative? The BW detractors [6] claim that BW have merely misquoted and misused the SP—making their experiment pointless. BW insist that their experiment exposes a flaw in SIQM [3–5].

Where do BW and their detractors agree? They agree that the null result of the experiment is a foregone conclusion. Why do they agree? Because, it is obvious that the position of the slit covers cannot really be uncertain in any quantum-mechanical sense. Their positions are “given away” by several easily measured phenomena, the most obvious being thermal radiation.

Where do BW and their detractors disagree? At the core of the dispute is the question of whether the experimenter can prevent state vector reduction by ignoring information. That is, by choosing not to perform obvious measurements. There are numerous recent examples of experiments in which interesting effects are obtained by choosing not to measure state vectors at some intermediate point in the experiment [7–11]. But it is obvious that one cannot choose to ignore arbitrarily large numbers of photons. It is unclear whether SIQM provides a prescription for deciding how many and what kind of photons (or other particles) can legitimately be ignored.

There is another line of inquiry suggested by the BW experiment. We propose to devise an experimental configuration in which the state vector of the movable slit covers (or their equivalent) is not given away by thermal radiation or any other effect, and the superposition effect we are trying to measure is not swamped by extraneous phenomena. These conditions could produce a non-null experimental outcome.

II. MODIFIED BW EXPERIMENT

Our objective at this stage is to use the BW setup to develop the tools and language to analyze the conjectured non-null experiment. We add to the BW apparatus a source of short wavelength radiation (λ_2) that can be used to probe the state (A open versus A closed) of the system, as shown in Figure 2.

If we just run the λ_1 part of the experiment, and if we take the superposition state $\frac{1}{\sqrt{2}}(|Ab\rangle + |aB\rangle)$ at face value then we get a λ_1 double-slit pattern. Next we observe the following sequence:

1. Turn on the λ_1 source and observe the double-slit pattern. Turn on the λ_2 source. (For clarity and simplicity, we can choose to use just one λ_2 particle.) As soon as D_{λ_2} either detects or fails to detect the λ_2 particle, the λ_1 double-slit pattern must vanish.

If we were to turn on the λ_1 source only after the λ_2 particle has encountered (or failed to encounter D_{λ_2} , then obviously there will be no λ_1 double slit-pattern.

Now we introduce the following wrinkle:

- 1'. First turn on E_{λ_2} , but instead of placing D_{λ_2} just beyond the A slit, allow the λ_2 particle to follow a long path to a distant mirror and then bounce back to be detected in the lab (Figure 3). (Note that we can set this up for both the transmitted and reflected paths or just one or the other.) Turn on E_{λ_1} , while the λ_2 particle is in flight to the distant mirror(s). Now we ask, “Does a λ_1 double-slit pattern appear while the λ_2 particle is in flight?”

Before answering, let us review the time-line of the experiment, as shown in Figure 4.

- t_0 — λ_2 emission
- t_1 — λ_2 encounter with SS
- t_2 — λ_1 emission
- t_3 — λ_1 encounter with SS
- t_4 — λ_1 encounter with double slit interference screen
- t_5 — λ_2 reflection
- t_6 — λ_2 detection

Now suppose that a λ_1 double-slit pattern is observed at t_4 . A λ_2 detection event at t_6 tells us that the A slit was either open or closed (not in the state $\frac{1}{\sqrt{2}}(|Ab\rangle + |aB\rangle)$) at time t_1 , so that λ_1 double-slit interference cannot occur at time $t > t_1$. This is not a paradox—it is a flat out contradiction.

Now suppose that a double-slit pattern is not observed at t_4 . The experimenter (who is presumably none other than Wigner’s friend) can then choose during the interval $t_4 < t < t_6$ to deactivate the λ_2 detectors. If the λ_2 particle floats away without being detected, then the λ_1 double-slit pattern *should* be observed—again a contradiction.

For completeness, we need to dispose of one other point. The reader has probably thought of something like the following rejoinder:

State vector reduction does not occur until time t_6 ; therefore, at time t_2 , the λ_1 quanta have equal probability of passing through A or B and can produce an interference pattern without contradicting detection of the λ_2 particle at D_{λ_2} at time t_6 .

We can refute this rejoinder with a simple example. Suppose that particle P_1 is subjected to a 50/50 quantum bifurcation. Its wave function becomes

$$|P_1\rangle = \frac{1}{\sqrt{2}}(|P_1\rangle_+ + |P_1\rangle_-). \quad (2)$$

Following the rejoinder, one can then argue that a second particle P_2 can be scattered off $|P_1\rangle_+$ even if a later measurement finds P_1 in $|P_1\rangle_-$.

Clearly, the rejoinder in this form is neither a sound argument, nor a proper expression of SIQM. Nevertheless, we can see a glimmer of something deeper if we continue in the direction the rejoinder leads us. It seems that the λ_1 and λ_2 observations should yield mutually compatible sets of basis vectors for the same Hilbert space. But the usual linear mapping works only in one direction, $|\lambda_1\rangle_{\text{interference}} = \frac{1}{\sqrt{2}}(|\lambda_2\rangle_{A\text{ open}} + |\lambda_2\rangle_{B\text{ open}})$. There are no expressions

$$\begin{aligned} |\lambda_2\rangle_{A\text{ open}} &= |\lambda_1\rangle_{\text{interference}} + \text{other vectors,} \\ |\lambda_2\rangle_{B\text{ open}} &= |\lambda_1\rangle_{\text{interference}} + \text{other vectors,} \end{aligned}$$

a fact to which we will return in the Conclusions (Section VII).

Now we need to come up with a more realistic superposition state and see what happens to this contradiction.

III. INTERFERENCE FROM A MESOSCOPIC MIRROR

We start with a mesoscopic mirror whose wave function is bifurcated. (That is, the mirror appears in one of two possible positions with a 50/50 probability. The wave function for positions in between is zero.)

Both the λ_1 and λ_2 photons are reflected by the mirror. This interval $t_3 - t_1$ must be kept very short, so that the recoil of the mirror from the λ_2 impact is minimized. Figure 5 shows the experimental setup with the two possible positions of the mirror separated by the distance $\frac{1}{4}\lambda_1$. It is evident from Figure 5 that there is an interference node for the reflected λ_1 photons. We therefore can develop the same kind of consistency argument as in Section II.

But is it really possible to prepare the mirror in such a state? We could use a half-silvered mirror, which bifurcates photon wave functions and so can in principle bifurcate its own wave function by interacting with a single photon.

The uncertainty in the mirror velocity from single photon bifurcation (SPB) with photon wavelength λ is

$$\Delta v_{SPB} = \frac{h}{\lambda M}. \quad (3)$$

Let us compare this with the velocity uncertainty due to wave packet spreading. In the initial state of the mirror, it is trapped with a small Gaussian uncertainty Δq_i . If the mirror is then released and its wave function allowed to spread, the characteristic initial spreading velocity Δv_i is

$$\Delta v_i = \frac{h}{4\pi\Delta q_i M}, \quad (4)$$

so

$$\frac{\Delta v_{SPB}}{\Delta v_i} = \frac{4\pi\Delta q_i}{\lambda}. \quad (5)$$

In our opinion, in a realistic experimental setup, $\lambda \gg \Delta q_i$ and hence $\Delta v_i > \Delta v_{SPB}$.

For our purposes, it is more difficult to work with the Gaussian distribution associated with Δv_i than to work with a bifurcated state, but it is not impossible. Note incidentally that if we work with Δv_i , we have no need of a triggering event.

Let us confine the mirror in a potential well U (see the appendix for the mechanism of the well) whose center is at $z = 0$ so that for suitably small z , U is approximated by $U = \frac{1}{2}kz^2$. This gives us a harmonic oscillator with mass M (the mass of the mirror). The essence of our scheme is to trap the mirror in the well and then dissipate energy until the ground state of the oscillator is reached. We then have

$$\frac{1}{2}k(\Delta q_i)^2 = \frac{1}{2}M(\Delta v_i)^2, \quad (6)$$

where Δq_i and Δv_i are the initial position and velocity uncertainty at the start of the experiment. We begin the experiment by turning off U , so that the center of mass wave function begins to spread with characteristic velocity Δv_i . We must demonstrate that

1. Δv_i is really the dominant effect, and
2. the λ_1 and λ_2 inconsistency argument can be brought to bear without using the especially advantageous bifurcation superposition of the mirror wave function.

IV. EXPERIMENTAL GEOMETRY

We must now lay out the geometry that will lead to the kind of inconsistency we are seeking. We will perform the analysis to first order; that is, neglecting the small amplitude attenuation due to differences in the propagation distance.

Consider a double slit experiment for λ_1 (Figures 6 and 7), in which the slits and the interference screen/detection system are each $\frac{5}{2}\lambda_1$ from the mirror. The distance between the slits is set at $2.29\lambda_1$, so that the distance between the right and left first nodes is also $2.29\lambda_1$. The mirror is circular, with diameter $\frac{5}{2}\lambda_1$.

z_m	$+\lambda_1$	0	$-\lambda_1$
$PL\Delta$	$0.77\lambda_1$	$0.50\lambda_1$	$0.36\lambda_1$

TABLE I. Values of $PL\Delta$ for different mirror positions.

We allow the wave function of the mirror to spread until $\Delta q = \lambda_1$. The path length difference ($PL\Delta$) between light from the far slit and the near slit is $\frac{1}{2}\lambda_1$ at the first node when the mirror is in its initial position ($z_m = 0$). We must compare this with the $PL\Delta$ for the mirror positions $z = \pm\lambda_1$. The results are given by Table I.

We see from Table I that for $z_m = \pm\lambda_1$, the position of the first node is substantially shifted. If the reflected λ_1 wave functions are based on superpositions of light reflected by the mirror from the positions smeared out over a $\Delta q = \lambda_1$ Gaussian distribution, the nodes at $x = \pm 1.145\lambda_1$ will be measurably less distinct than if z_m is fixed at 0. *This is the crucial effect that we need to observe.*

The third step in the setup of our experiment is the introduction of the λ_2 photons. As in Section II, the λ_2 photons are used to measure the mirror's position. The λ_2 quanta, in plane wave form, pass through an aperture of width W_a and are incident on the mirror at a shallow angle θ . They are reflected at the same angle to the D_{λ_2} detector. Setting $W_a = 4\lambda_2 \cos \theta$, we see that a detection event at D_{λ_2} determines that the mirror position was in the range

$$|z_m| \leq \frac{W_a}{4 \cos \theta} = \lambda_2. \quad (7)$$

If we set $\lambda_2 = \frac{1}{4}\lambda_1$, then

$$|z_m| \leq \frac{1}{4}\lambda_1. \quad (8)$$

This condition leads to a much narrower range of values for $PL\Delta$ than those given in Table I. If (8) is satisfied, the interference node is then resharpened (Figure 8). This resharpening then leads to the same inconsistency as in Section II. Figure 9 shows the complete apparatus for this modified BW experiment based on a mesoscopic mirror with wave packet spreading.

V. INTERFERENCE PATTERNS

The interference effects on which this experiment is based are rather subtle, so they must be treated carefully. Coherent light emerges from two pointlike slits, A and B. The photons rebound off the wave function of the mirror and interfere on a screen between the slits. The details of the interference pattern vary, depending upon the mirror's wave function.

The E field for the light from slit A at a point D away from that slit is given by

$$E_A = K \int P(z) \cos \left[\frac{4\pi}{\lambda_1} \sqrt{\left(z + \frac{5}{2}\lambda_1 \right)^2 + D^2/4} \right] dz, \quad (9)$$

where $P(z) = |\psi(z)|^2$ is the probability density for the mirror's position and K is a scaling factor. The separation between the two slits (which should be close to $2.29\lambda_1$) is S . For slit B, the expression is similar,

$$E_B = K \int P(z) \cos \left[\frac{4\pi}{\lambda_1} \sqrt{\left(z + \frac{5}{2}\lambda_1 \right)^2 + (S - D)^2/4} \right] dz. \quad (10)$$

The probability density is $P(z) = \delta(z)$ if the mirror's position is fixed. For the Gaussian wave packet, the probability density is

$$P(z) = \sqrt{\frac{1}{2\pi\lambda_1^2}} e^{-z^2/2\lambda_1^2}. \quad (11)$$

The magnitude of the observed interference pattern is just given by the intensity,

$$I = \frac{1}{2}(E_A + E_B)^2. \quad (12)$$

Since both E_A and E_B are functions of D , I is a function of D as well. The variation in I in the range $0 < D < S$ gives us the interference effect.

Figure 8 shows the actual interference patterns generated by two different wave functions, with the slit separation set to $S = 2.3\lambda_1$. In the first, the wave function is the Gaussian (11). In the second, that wave function has been truncated to the region $|z_m| \leq \frac{1}{4}\lambda_1$. The interference fringes at the edges are much sharper for the truncated wave function, as is needed to produce the contradiction.

We have so far treated the experimental geometry as if z motion were the only wave packet spreading that occurs. There is other movement that can spoil the experiment if not dealt with. First, let us consider sideways drift of the mirror in the xy -plane. Conceptually, the simplest way to deal with this is to have an “out of position” sensing system made of beams and detectors. We then make a large number of experimental runs and use only the data obtained when the mirror is not “out of position.”

More difficult is tilting of the mirror out of the xy -plane. There are two methods for dealing with this. The preferred method would be gyroscopic stabilization by rotation in the xy -plane. This must certainly be used in the process of trapping and confining the mirror (Appendix A) that precedes the experiment proper. But we need to be careful about this, as too rapid motion could cause difficulties. The second method involves a beam and detectors. The beam is incident perpendicular to the mirror's initial position and $\lambda_{beam} \ll \lambda_1$, so, regardless of interference or reduction, the beam provides negligible information about z_m . The recoil velocity of the mirror from the beam impact is relatively large, but as with λ_2 , the beam impact is timed just before t_3 , so the recoil distance is small.

VI. RESTRICTIONS ON EXPERIMENTAL CONDITIONS

We have discussed the geometry of the λ_1, λ_2 inconsistency using only the relative values of λ_1, λ_2 , and W . We must now demonstrate that this is the dominant effect for some values of λ_1, M , and Δq_1 . We start by considering the problem of *radiation* from the mirror. This can ruin the experiment by “giving away” the mirror's position.

In order to get numerical results, we have used parameters for Vanadium:

$$\begin{aligned} \text{density} &= \rho = 6.1 \text{ g/cm} \\ \text{speed of sound} &= v_s = 3 \times 10^5 \text{ cm/s} \\ \text{atomic weight} &= a_w = 50 \text{ amu} \\ \text{lattice spacing} &= d = 2.4 \times 10^{-8} \text{ cm.} \end{aligned}$$

More importantly, we have to choose a value for λ_1 . The one that seems to work best is 10^{-6} cm. For photons, this would mean x-rays. At x-ray wavelengths, simple geometric reflection breaks down, since the frequency of the incoming radiation nears the plasma frequency of the mirror. So instead of photons, we will need to use ~ 1 keV electrons, which do reflect properly from the mirror surface.

Many photons whose total energy is E_T give less position information than a single photon with energy

$$E_T = \frac{hc}{\lambda}. \quad (13)$$

So we set

$$E_T = \frac{hc}{W} = \frac{hc}{\frac{5}{2}\lambda_1}, \quad (14)$$

and also set E_T equal to the thermal output of the mirror during time $t_s = \frac{\lambda_1}{\Delta v_i}$, the time necessary for the spreading to reach λ_1 :

$$E_T = t_s e \sigma T^4 \left[2\pi \left(\frac{5}{4} \lambda_1 \right)^2 \right] \quad (15)$$

so

$$\frac{hc}{\frac{5}{2}\lambda_1} = \frac{\lambda_1}{4\Delta v_i} e \sigma T^4 \left[2\pi \left(\frac{5}{4} \lambda_1 \right)^2 \right], \quad (16)$$

which reduces to

$$T^4 = \frac{1}{t_s} \frac{1}{e \sigma} \frac{hc}{\frac{1}{2}\pi \left(\frac{5}{2} \lambda_1 \right)^3}. \quad (17)$$

Since

$$t_s = \frac{\lambda_1}{\Delta v_i} = \frac{4\pi \Delta q_i M \lambda_1}{h}, \quad (18)$$

we see that

$$T^4 = \frac{h^2 c}{e \sigma} \frac{1}{2\pi \Delta q_i M \left(\frac{5}{2} \right)^3 \lambda_1^4},$$

or

$$T^4 = \frac{2.6 \times 10^{-35}}{\lambda_1^6 \Delta q_i}. \quad (19)$$

To evaluate (19) we need to make a decision about what value of Δq_i to use. This is probably the hardest parameter to pin down without actually performing the experiment, but the natural choice seems to be

$$\Delta q_i = \frac{1}{2}d, \quad (20)$$

which in this case is 1.2×10^{-8} cm. Then using $\lambda_1 = 10^{-6}$ cm, we get:

$$\begin{aligned} \Delta v_i &= 3.8 \times 10^{-3} \text{ cm/s}, \\ t_s &= 2.6 \times 10^{-4} \text{ s}, \\ M &= 1.1 \times 10^{-17} \text{ g, and} \\ T_R &= 2.2 \times 10^2 \text{ K.} \end{aligned}$$

We will subsequently find that there are other temperature limits more stringent than this. But this limit is conceptually important, because it is the temperature below which we can treat the mirror as an independent system.

The main phenomenon that competes with wave packet spreading in determining the initial velocity is thermal motion *within* the mirror. At very low temperature, thermal energy in the mirror is stored in the lowest frequency phonons available—the lowest harmonics of the disk.

We can find the temperature cut-off where the two competing effects are roughly equal by equating the total momenta

$$(\mu v_s) \sqrt{2} = M \Delta v_i, \quad (21)$$

where $\mu \equiv$ reduced mass $\approx \frac{1}{2}M$. From this, it follows that

$$\frac{1}{2} \mu v_s^2 = \frac{1}{2} M (\Delta v_i)^2. \quad (22)$$

But $\frac{1}{2} \mu v_s^2$ is half the thermal energy in each mode, which is also

$$E = \frac{\hbar \omega / 2}{e^{\hbar \omega / k_B T} - 1}; \quad (23)$$

therefore, at T_c we have

$$\begin{aligned} \frac{1}{2} M (\Delta v_i)^2 &= \frac{\hbar \omega / 2}{e^{\hbar \omega / k_B T_c} - 1} \\ \ln \left[\frac{\hbar \omega}{M (\Delta v_i)^2} + 1 \right] &= \frac{\hbar \omega}{k_B T_c}, \end{aligned} \quad (24)$$

so

$$T_c = \frac{\hbar\omega}{k_B} \left(\ln \left[\frac{\hbar\omega}{M(\Delta v_i)^2} + 1 \right] \right)^{-1}. \quad (25)$$

From the geometry of the problem, we can see that $\omega = \frac{2\pi v_s}{\lambda}$, where λ is now the diameter of the mirror disk, so for an arbitrary value of λ_1 ,

$$\omega = \frac{2\pi v_s}{\frac{5}{2}\lambda_1} = \frac{4\pi}{5} \frac{v_s}{\lambda_1} = \frac{7.5 \times 10^5}{\lambda_1}. \quad (26)$$

So our value of T_c becomes

$$T_c = (5.7 \times 10^{-6})[\lambda_1 \ln \lambda_1 (1.1 \times 10^{12})]^{-1}. \quad (27)$$

For $\lambda_1 = 10^{-6}$ cm,

$$T_c = 4.1 \times 10^{-1} \text{ K}. \quad (28)$$

Below T_c , wave packet spreading dominates the effect of thermal phonons within the mirror.

Now consider the thermal conditions outside the mirror. In order to trap the mirror in a potential well before the beginning of the experiment proper, the mirror needs to start with a very small thermal velocity—not too much greater than Δv_i . Approximating by the ideal gas value,

$$\frac{1}{2}Mv_T^2 = \frac{3}{2}k_B T_g, \quad (29)$$

we get

$$v_T = 6.2\sqrt{T_g} \text{ cm/s}. \quad (30)$$

If we set $v_T = \alpha \Delta v_i$, then

$$T_g = 3.8 \times 10^{-7} \alpha^2 \text{ K}. \quad (31)$$

For $\alpha < 10^3$, (31) is a much tighter restriction than (28). Part of our experimental strategy would be to use a sequence of trapping maneuvers to raise the allowable values of α and T_g . One of these maneuvers would be likely to involve attaching the mirror to a more massive object using macromolecules that can change their tertiary structure [12,13].

We also require that the density of the gas surrounding the mirror be low enough so that there will be no collisions during the time t_s . This means that there must be less than one molecule in the volume

$$V = (v_g t_s) \pi \left(\frac{5}{4} \lambda_1 \right)^2, \quad (32)$$

where v_g is the rms velocity of the gas molecules at temperature T_g . For Rubidium (frequently used in Bose-Einstein condensate experiments),

$$v_g = 1.06 \alpha \text{ cm/s}, \quad (33)$$

and

$$V = 1.33 \times 10^{-15} \alpha \text{ cm}^3. \quad (34)$$

This yields a density of

$$\rho_\alpha = \frac{1.2 \times 10^{-6}}{\alpha} \text{ mole/L.} \quad (35)$$

Note that if $\rho \ll \rho_\alpha$, the mirror will sometimes approach the trap with a Brownian velocity

$$v_{Br} < v_T = \alpha \Delta v_i. \quad (36)$$

Taking full advantage of this, we should be able to work at values of $\alpha > 5$ and hence $T_g > 10 \mu\text{K}$.

VII. CONCLUSIONS

We have designed an experiment that must have a consistent outcome. The outcome can certainly be consistent if desharpening of the λ_1 nodes is not found to occur. But then quantum mechanics does not correctly predict the λ_1 pattern. If we want to retain quantum mechanics, λ_1 desharpening should occur. Then, to avoid the Wigner's friend contradiction, we are forced to jettison SIQM and take another path.

The λ_1 pattern must be unaffected by λ_2 detection, even though λ_2 detection restricts the mirror to $|z_m| \leq \frac{\lambda_1}{4}$. This means that λ_1 develops the desharpened $|z_m| < \lambda_1$ -related nodes without encountering the mirror in the zone \mathcal{Z} where $\lambda_1 > |z_m| > \frac{\lambda_1}{4}$. Presumably, this is pretty much what happens with or without λ_2 . λ_1 must encounter the mirror itself only in a small region $\Delta z \ll \lambda_1$, and in most of the larger region, $|z_m| < \lambda_1$, it will encounter some kind of signal from the mirror. This signal cannot reflect the λ_1 wave, but it can modulate the wave to produce the correct interference pattern if

1. the mirror emits the signal continuously, like the wake of a boat, and
2. the signal contains enough information about the evolution of the state of the mirror.

Note that although the linear wave equation correctly predicts the shape of the λ_1 nodes, the underlying process, with propagation of the modulating signal taking the place of wave packet spreading, is fundamentally nonlinear.

Let us now consider the experiment from a mathematical point of view. We find that there is a “duality” of λ_2 position measurement: λ_1 reflection interference. We already know that this duality does not operate in the usual manner to produce two different sets of basis vectors for the same space. Instead, the λ_1 and λ_2 measurements lead us to two different

vector spaces, that presumably are tangent in some sense to the (infinite-dimensional) manifold that actually represents the state of the system. The superposition principle hold only within these individual vector spaces.

It is natural to conjecture that this duality is a special case of a multiplicity of distinct properties and corresponding vector spaces, each of which is accessed by a different probe of the mirror system. Ordinarily, each probe disrupts all the others to such an extent that the multiplicity is not evident.

Consider the information-carrying signal in this light. The signal exists in the space that describes the experiment but not in the “tangent” spaces that are the setting for SIQM. The signal is able to correctly modulate λ_1 , because it carries *locally* information about phase correlations that occur elsewhere. Such richness of information content is possible only if the signal dwells in a very large and profoundly non-linear space.

The effects we have described can exist only under extreme conditions of low temperature with very careful state preparation. They are nevertheless based on rather general features of wave mechanics. The necessary temperature regime is now accessible to experimentalists. We believe that an experiment of this type can be performed, although it probably would entail the use of states more specifically tailored to micro-Kelvin conditions.

APPENDIX A: TRAPPING, CONFINING, AND RELEASING THE MIRROR TO START THE EXPERIMENT

We propose to trap the mirror by floating it in a magnetic field balanced by a weak fictitious gravitational field due to an acceleration. The magnetic field would induce a superconduction current in the mirror. The x and y components of the \vec{B} field will then act on the current to produce a force opposite to the fictitious force. The mirror will sit in a potential well approximately given by

$$\frac{1}{2}kz_m^2 = \frac{1}{2}Mv^2 \quad (\text{A1})$$

In particular, k must satisfy

$$\frac{1}{2}k(\Delta q_i)^2 = \frac{1}{2}M(\Delta v_i)^2, \quad (\text{A2})$$

so

$$k = 1.1 \times 10^{-6} \text{ erg/cm}^2 \quad (\text{A3})$$

and the oscillator frequency ω_{os} is

$$\omega_{os} = \sqrt{\frac{k}{M}} = 3.2 \times 10^5. \quad (\text{A4})$$

Let us calculate the magnitude of the \vec{B} field. We simplify the problem by replacing the mirror disk with a ring of radius λ_1 . Also,

$$B_z \approx B_0 \sin \omega t, \quad (\text{A5})$$

where $\frac{2\pi}{\omega} \gg t_s$, and

$$B_r \approx B_\perp \sin \omega t$$

$$B_\perp \approx \eta B_0, \quad (\text{A6})$$

where η is slowly varying with respect to z . Then from

$$\oint E \cdot ds = -\frac{1}{c} \frac{d\Phi_B}{dt} \quad (\text{A7})$$

we get

$$E(2\pi\lambda_1) = -\frac{1}{c} B_0 \pi \lambda_1^2 (\omega \cos \omega t) \quad (\text{A8})$$

$$E = -\frac{1}{2c} \lambda_1 B_0 \omega \cos \omega t. \quad (\text{A9})$$

This acts on superconducting electrons to produce

$$a = \frac{F}{m_e} = \frac{eE}{m_e} = -\frac{e\lambda_1}{2m_e c} B_0 \omega \cos \omega t, \quad (\text{A10})$$

and

$$v = -\frac{e\lambda_1}{2m_e c} B_0 \sin \omega t. \quad (\text{A11})$$

The the radial component of \vec{B} , B_r acts on each electron to produce a force

$$F_e = -\frac{ev}{c} B_r$$

$$F_e = \frac{e^2 \lambda_1}{2m_e c^2} B_0 B_\perp \sin^2 \omega t. \quad (\text{A12})$$

If there are ν Cooper pairs for each lattice position, and N is the total number of atoms in the mirror, then the total upward force on the mirror is

$$F_{EM} = N\nu\eta \frac{e^2 \lambda_1}{m_e c^2} B_0^2 \sin^2 \omega t. \quad (\text{A13})$$

Because $t_{EM} = \frac{2\pi}{\omega} \gg t_s$, we can time the experiment to be performed when F_{EM} is at its maximum,

$$F_{EM\text{-max}} = N\nu\eta \frac{e^2 \lambda_1}{m_e c^2} B_0^2. \quad (\text{A14})$$

The balancing acceleration would have the same periodicity as F_{EM} . The potential well is created by the inhomogeneity inhomogeneity of the \vec{B} field as a function of z .

$$H_{total} = \int F_{EM} dz - F_{accel} z. \quad (\text{A15})$$

So we have

$$H_{total\text{-max}} = \int F_{EM\text{-max}} dz - F_{accel\text{-max}} z$$

$$H_{total} \approx \frac{1}{2} \frac{\partial F_{EM\text{-max}}}{\partial z} z^2, \quad (\text{A16})$$

so we can see that

$$k \approx \frac{\partial F_{EM}}{\partial z} \approx 2N\nu\eta \frac{e^2 \lambda_1}{m_e c^2} B_0 \frac{\partial B_0}{\partial z}. \quad (\text{A17})$$

Therefore, $B_0 \frac{\partial B_0}{\partial z} \approx \frac{k m_e c^2}{2 N \nu \eta e^2 \lambda_1} \approx \frac{1.8 \times 10^7}{\nu \eta}$. If we set $\nu = 10^{-3}$ and $\eta = 10^{-1}$, then $B_0 \frac{\partial B_0}{\partial z} \approx 1.8 \times 10^{11}$. If B_0 varies by about 25 percent over the distance λ_1 in the vicinity of the mirror, then

$$\begin{aligned} \frac{\partial B_0}{\partial z} \lambda_1 |_{z=0} &\approx \frac{1}{4} B_0 |_{z=0} \\ B_0 \frac{\partial B_0}{\partial z} |_{z=0} &\approx \frac{B_0^2}{4 \lambda_1}. \end{aligned} \quad (\text{A18})$$

This reduces to $B_0 |_{z=0} \approx 8.5 \times 10^2$ G.

Finally, the mirror is released by turning off the field over a time scale t_R that satisfies

$$t_R \ll t_s. \quad (\text{A19})$$

Ideally, one would also want

$$t_R < \frac{2\pi}{\omega_{os}}. \quad (\text{A20})$$

The mirror would be briefly exposed to a strong \vec{E} field during the turn-off.

REFERENCES

- [1] D. Bedford, D. Wang, Found. of Phys. **6** 599 (1976).
- [2] D. Bedford, D. Wang, Nuovo Cimento B **32** 243 (1976).
- [3] D. Bedford, D. Wang, Nuovo Cimento B **26** 313 (1975).
- [4] D. Bedford, D. Wang, Nuovo Cimento B **37** 55 (1977).
- [5] D. Bedford, D. Wang, Found. of Phys. **13** 987 (1983).
- [6] D. Guthkovski, M. V. Valdes Franco, Found. of Phys. **13** 963 (1983).
- [7] L. J. Wang, X. Y. Zou, L. Mandel, J. Opt. Soc. Am. B **8** 978 (1991).
- [8] L. J. Wang, X. Y. Zou, L. Mandel, Phys. Rev. A **44** 4614 (1991).
- [9] L. J. Wang, X. Y. Zou, L. Mandel, Phys. Rev. Lett. **67** 318 (1991).
- [10] Z. Y. Ou, L. J. Wang, L. Mandel, Phys. Rev. A **40** 1428 (1989).
- [11] Z. Y. Ou, L. J. Wang, L. Mandel, Phys. Rev. A **41** 1597 (1990).
- [12] J. Terner, J. D. Stong, T. G. Spiro, M. Nagumo, M. F. Nicol, M. A. El-Sayed, in *Hemoglobin and Oxygen Binding*, edited by C. Ho (Elsevier, New York, 1982).
- [13] B. Alpert, L. Lindqvist, S. El Mohsni, F. Tfibel, in *Hemoglobin and Oxygen Binding*, edited by C. Ho (Elsevier, New York, 1982).

FIG. 1. The Bedford-Wang experiment. D detects the trigger photon (ψ_{TP}), then sends a signal to the mechanical linkage (ML), which moves the slit covers from $|Ab\rangle$ to $|aB\rangle$.

FIG. 2. Apparatus shown in A open, B closed configuration (state $|Ab\rangle$). Note that the λ_2 beam and detector can be tilted slightly out of the xy -plane to avoid confusion.

FIG. 3. The apparatus modified for a long excursion taken by the λ_2 photons.

FIG. 4. Time-line of the Gedanken experiment.

FIG. 5. A bifurcated mirror generating a simple interference pattern. The z_1 reflected wave and the z_2 reflected wave are out of phase by π at the center of the pattern.

FIG. 6. Reflection off a mirror of diameter $\frac{5}{2}\lambda_1$. The two paths arrive at the interference screen out of phase by π ; however, they do not exactly cancel, because the the amplitude decays along paths of differing lengths. To avoid confusion between the outgoing and reflected λ_1 quanta, the beam is tilted slightly out of the xz -plane.

FIG. 7. The range of paths that the reflected quanta may take, for a mirror with a spread of $\Delta z = \lambda_1$.

FIG. 8. Interference patterns for a mirror with a Gaussian wave packet with $\Delta z = \lambda_1$ and one for which the same Gaussian has been truncated to $\pm\frac{\lambda_1}{4}$.

FIG. 9. The configuration for the non-null experiment. Shown are the λ_1 and λ_2 paths corresponding to the extreme mirror positions permitted by a D_{λ_2} detection event.

This figure "dgrm1.jpg" is available in "jpg" format from:

<http://arxiv.org/ps/quant-ph/9905030v1>

This figure "dgrm2.jpg" is available in "jpg" format from:

<http://arxiv.org/ps/quant-ph/9905030v1>

This figure "dgrm3.jpg" is available in "jpg" format from:

<http://arxiv.org/ps/quant-ph/9905030v1>

This figure "dgrm4.jpg" is available in "jpg" format from:

<http://arxiv.org/ps/quant-ph/9905030v1>

This figure "dgrmb5.jpg" is available in "jpg" format from:

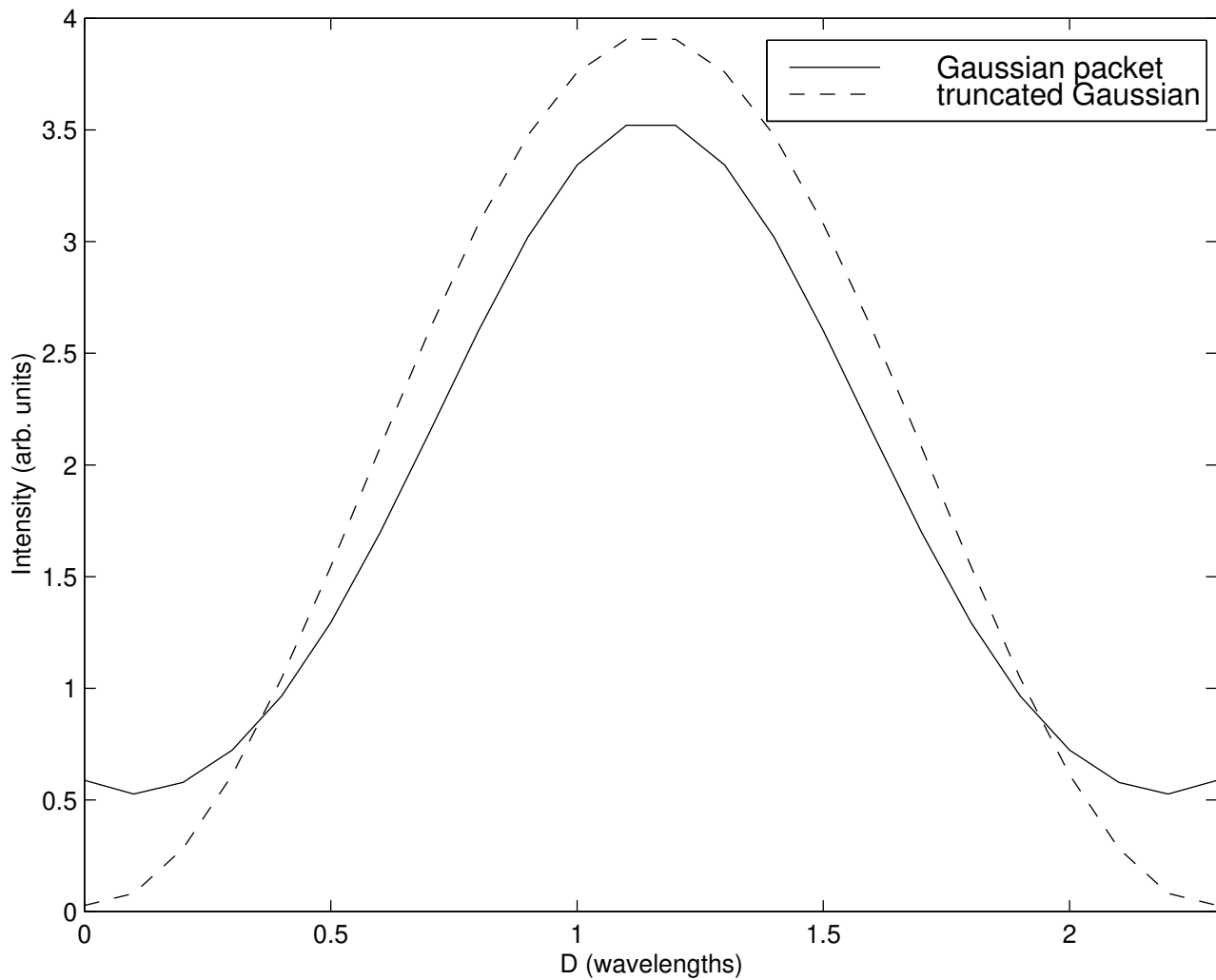
<http://arxiv.org/ps/quant-ph/9905030v1>

This figure "dgrmb6.jpg" is available in "jpg" format from:

<http://arxiv.org/ps/quant-ph/9905030v1>

This figure "dgrmb7.jpg" is available in "jpg" format from:

<http://arxiv.org/ps/quant-ph/9905030v1>



This figure "dgrmb9.jpg" is available in "jpg" format from:

<http://arxiv.org/ps/quant-ph/9905030v1>